Applied Energy 228 (2018) 1136–1146

Contents lists available at ScienceDirect

Applied Energy

journal homepage: www.elsevier.com/locate/apenergy

On the temporal modelling of solar photovoltaic soiling: Energy and economic impacts in seven cities

Siming You[a], Yu Jie Lim[b], Yanjun Dai[c], Chi-Hwa Wang[b,*]

[a] Division of Systems, Power & Energy, School of Engineering, University of Glasgow, G12 8QQ Glasgow, UK
[b] Department of Chemical and Biomolecular Engineering, National University of Singapore, Singapore 117585, Singapore
[c] School of Mechanical Engineering, Shanghai Jiao Tong University, Shanghai 200240, China

HIGHLIGHTS

- The energy and economic impacts of solar photovoltaic soiling were modelled.
- Relative net-present value change was defined to assess optimal cleaning intervals.
- We compared the soiling-induced efficiency and economic losses in seven cities.
- The efficiency loss is the lowest (< 0.04) for Tokyo and highest (> 0.8) for Doha.
- The optimal intervals are 23–70 days (manual) and 17–49 days (machine).

ARTICLE INFO

Keywords:
Solar PV
Soiling
Energy loss
Economics
Cleaning
Renewable energy

ABSTRACT

This work developed a framework to predict the energy and economic impacts of solar photovoltaic soiling. This framework includes the effects of relative humidity, precipitation and tilt angle on solar photovoltaic soiling. A concept of relative net-present value change was introduced to determine the optimal cleaning interval. The uncertainties in the economic analysis were accounted for using a Monte Carlo simulation method. The framework was used to study the soiling-induced efficiency and economic losses of solar photovoltaic modules in seven cities (*i.e.* Taichung, Tokyo, Hami, Malibu, Sanlucar la Mayor, Doha, and Walkaway). Overall, the efficiency loss (in ascending order) for Tokyo/Walkaway < Taichung < Sanlucar la Mayor < Malibu/Hami < Doha for a one-year study period. Doha experiences an efficiency loss over 80% for a 140-day exposure, while Tokyo has an efficiency loss less than 4% for a one-year exposure. Malibu has longest optimal cleaning intervals (70 days for manual cleaning and 49 days for machine-assisted cleaning) that leads to the relative net-present value changes of 1.7% and 1.1%. Doha has the shortest optimal cleaning intervals (23 days for manual cleaning and 17 days for machine-assisted cleaning) that leads to the relative net-present value changes of 21% and 19%. The work serves as an effective tool for designing optimal cleaning protocols for solar photovoltaic systems.

1. Introduction

World energy consumption was projected to increase by 28% between 2015 and 2040 in accordance with the rapid growth in electricity demand and economy [1]. Limited reserves of fossil fuels and widespread concerns over greenhouse gas (GHG) emissions from fossil fuel consumption stimulate extensive research in renewable energy development. As a major form of renewable energy, solar photovoltaic (PV) electricity generation has drawn an ever-increasing attention due to its abundance, accessibility, and technical maturity [2].

However, solar PV systems are plagued by the issue of natural soiling whereby particulate matters (PM) accumulate on the surface of solar PV panels, resulting in light transmission blockage and irradiance reduction. The solar conversion efficiency of solar PV modules could be lowered by 4–25% due to the soiling [3–5]. Piliougine et al. [6] found that an average daily energy loss of 2.5% was resulted by soiling. Solar PV soiling is especially a concern for the regions where there are frequent sandstorms or haze episodes [7]. This issue could also be exacerbated during dry seasons when there is insufficient rainfall to clean PV surfaces [8]. The soiling-induced efficiency reduction not only adversely affects the stability and overall energy performance of solar PV systems but also incurs additional economic and logistics requirements

* Corresponding author.
E-mail address: chewch@nus.edu.sg (C.-H. Wang).

https://doi.org/10.1016/j.apenergy.2018.07.020
Received 31 March 2018; Received in revised form 24 June 2018; Accepted 5 July 2018
Available online 07 July 2018

Nomenclature

C_D	drag coefficient
C_{DS}	surface drag coefficient
C_c	Cunningham correction factor
C ($\mu g \cdot m^{-3}$)	atmospheric aerosol concentration
C_1, C_2, C_3, C_4	empirical constants
d_p (m)	particle diameter
D ($m^2 s^{-1}$)	Brownian diffusion coefficient
g ($m \cdot s^{-2}$)	gravitational acceleration
h (m)	reference height
k (JK^{-1})	Boltzmann constant
LT	life time of facilities
NPV (USD)	net-present value
ΔNPV%	relative NPV change
R_{at} ($s \cdot cm^{-1}$)	atmospheric turbulence resistance term
R_b ($s \cdot cm^{-1}$)	quasi-laminar resistance term
Re_p	particle Reynolds number
r_d (m)	dry particle radius
r_w (m)	wet particle radius
r	discount rate
Sc	Schmidt number
St	Stokes number
T (K)	air temperature
U ($m \cdot s^{-1}$)	mean wind velocity
u_* ($m \cdot s^{-1}$)	friction velocity
V_s ($m \cdot s^{-1}$)	sedimentation velocity
V_d ($m \cdot s^{-1}$)	total deposition velocity
z_0 (m)	roughness length
ρ_f ($kg \cdot m^{-3}$)	density of fluid
ρ_p ($kg \cdot m^{-3}$)	density of aerosol particle
ρ_D ($g \cdot m^{-2}$)	dust deposition density
μ ($kg \cdot m^{-1} s^{-1}$)	viscosity of air
k	von Karman constant
ν ($m^2 s^{-1}$)	kinematic viscosity of air
θ (°)	solar PV tilt angle
η_{loss}	efficiency loss

upon solar PV cleaning [9]. Moreover, solar PV soiling has also becomes an important factor that needs to be considered during PV grid integration [10] and the evaluation of solar irradiation potential [11].

Particle deposition and accumulation on solar PV panels are affected by a variety of factors including relative humidity, wind speed, panel tilt angle, and rainfall. Under high relative humidity conditions, hygroscopic particles could be enlarged due to the absorption of environmental moisture [12]. The change in particle size could significantly affect the velocity of particle deposition [13]. Particle deposition also increases with the increase of wind speeds due to an enhanced effect of turbulent deposition [14]. The tilt of PV panels reduces particle deposition and thus the efficiency loss by soiling [15]. Elminir et al. found that the particle deposition density was 15.84 g/m^2 for a tilt angle of 0° and decreased to 4.48 g/m^2 for a tilt angle of 90° based on a seven-month experiment in Egypt [16]. Mejia and Kleissl found that the average soiling losses for a tilt angle smaller than 5° are five times of that for a tilt angle larger than 5° in California [17]. Lu and Zhao [18] found that the tilted angles of 25°, 40°, 140° and 155° corresponded to the maximum deposition rates of 14.28%, 13.53%, 6.79% and 9.78%, respectively.

To design effective protocols for solar PV cleaning, it is critical to understand the temporal impacts of solar PV soiling on the efficiency degradation of PV modules. Empirical models (*e.g.*, [19,20]) have been developed based on the regression analysis or artificial Neural Network modelling of experimental data of a specific region. These models have the advantages of being simple, straightforward, and easy to use. However, they are highly contingent upon existing experimental data and are hard to be applied to other regions with different environmental and meteorological conditions from the region where the model was based on. CFD simulation (*e.g.,* [21]) has also been used to study the process of solar PV soiling, which, however, has a high requirement on computational resources. As a promising alternative, mechanistic models could be developed by combining the prediction of particle deposition with the relationship between particle deposition density and solar PV efficiency loss. These models have the advantage of being applicable to a wide range of regions. One such model was proposed by [22] to estimate the cleaning frequency for dirty solar modules. However, this model was based on an empirical model for 'indoor' particle deposition [23] which are generally subject to different environmental conditions from outdoor particle deposition.

There is still lack of mechanistic models that are specifically designed to predict the temporal solar PV soiling under outdoor environmental conditions. Especially, such models need to be able to consider the effect of relative humidity on particle deposition. On the other hand, to develop an economically sustainable solar PV cleaning protocol, it is critical to predict the optimum cleaning interval or frequency from a system perspective. Existing studies estimated the optimum cleaning interval by matching the cleaning-related cost with the energy output loss by soiling [24]. This method, however, did not consider system-level economics and the time value of money. Hence, a system-level economic analysis is needed to evaluate the economics of cleaning plans, which has rarely been done but will allow investors to make informed decisions about when to conduct the cleaning to optimize the profitability of solar PV systems.

In this work, we propose a solar PV soiling prediction model based on the theoretical modelling of particle deposition. The effects of meteorological factors (*e.g.*, relative humidity and precipitation) on solar PV soiling are considered. The economic impacts of solar PV soiling and cleaning are evaluated based on a system-level economic analysis. The optimal cleaning interval is determined by minimizing the relative net-present value (NPV) change. The model is then used to predict and compare the soiling-induced efficiency and economic losses of solar PV modules in seven cities (*i.e.*, Taichung, Tokyo, Hami, Malibu, Sanlucar la Mayor, Doha, and Walkaway) where solar PV has been extensively deployed.

2. Methodology

2.1. Particle deposition model

Outdoor particle deposition could be considered to be driven by two mechanisms, *i.e.* gravitational settling as well as wind turbulence and boundary layer effects [25]. Correspondingly, the atmosphere beneath a convenient reference height (*e.g.*, 20 m) was segregated into two layers [26]: (a) an upper layer where particle transport was governed by an atmospheric turbulence resistance term and (b) an underlying quasi-laminar layer where particle transport was governed by Brownian diffusion and inertial impaction that could be grouped into a quasi-laminar resistance term. In this case, particle deposition could be modelled by a resistance in parallel model including two pathways, *i.e.* atmospheric turbulence and quasi-laminar layer mass transfer, and sedimentation (Fig. 1) [25].

The total deposition velocity V_d could be expressed as

$$V_d = \frac{1}{R_{at} + R_b} + V_s \cos\theta \quad (1)$$

where $R_{at} = \frac{1}{C_{DS} U}$ accounts for the atmospheric turbulence resistance term in the upper layer with C_{DS}being the surface drag coefficient and U

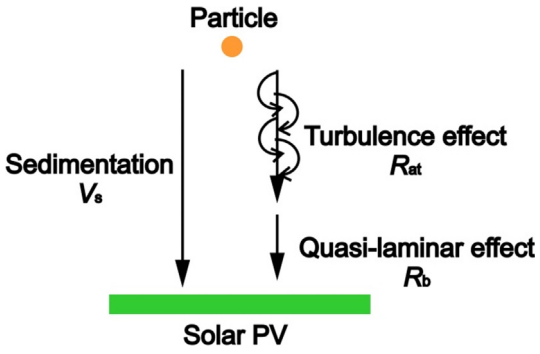

Fig. 1. A schematic of particle deposition model.

(ms^{-1}) being the mean wind velocity. C_{DS} accounts for the intense turbulence when the wind blows over rough surfaces such as land and is related to atmospheric stability and surface roughness [27,28]. C_{DS} has a global yearly average value of 1.2×10^{-2} over land and 1.2×10^{-3} over oceans [29]. The former will be used in this work. Wind speed is usually measured with an anemometer at a height of 10 m at weather stations according to the World Meteorological Organization [30]. Hence, a reference height of 10 m is considered for all wind speed reported unless otherwise stated. $C_{DS}U$ (ms^{-1}) represents the capability of wind to transfer kinetic energy to particles in the air. $R_b = \frac{1}{u_*\left[Sc^{-0.5} + \frac{St^2}{1+St^2}\right]}$ accounts for the quasi-laminar layer resistance which factors in processes like Brownian diffusion and inertial impaction. $\cos\theta$ is used to account for the effect of solar PV panel tilt as explained later.

u_* (ms^{-1}) is the friction velocity and is an indicator of atmospheric turbulence [31]. At neutral atmospheric conditions, u_* is calculated as [32]

$$u_* = \frac{\kappa U}{\ln\left(\frac{h}{z_0}\right)} \tag{2}$$

where $k = 0.41$ is the von Karman constant. $h = 10$ m is the reference height. $Z_0 = 1$ m is the roughness length for the case of urban land [33]. Sc is the Schmidt number defined as the ratio of momentum diffusivity and mass diffusivity, and is given as [34]

$$Sc = \frac{v}{D} \tag{3}$$

where v is the kinematic viscosity of air ($1.48 \times 10^{-5} m^2 s^{-1}$). D ($m^2 s^{-1}$) is the Brownian diffusion coefficient and calculated as

$$D = \frac{kTC_c}{3\pi\mu d_p} \tag{4}$$

where k is the Boltzmann constant ($1.38 \times 10^{-23} JK^{-1}$). T is the air temperature. C_c is the Cunningham correction factor. St is the Stokes number defined as the ratio of the characteristic time of particle to a characteristic time of the flow. It is calculated as [34]

$$St = \frac{(u_*)^2 V_s}{gv} \tag{5}$$

Gravitational settling is represented by the sedimentation velocity term (V_s). The suspension of aerosol particles in the air is dilute thus the particles are assumed to fall at their single particle terminal velocity [35]. V_s (ms^{-1}) is calculated by

$$V_s = \frac{\rho_p g d_p^2}{18\mu} \text{ for } Re_p \leqslant 1.0$$
$$V_s = \left(\frac{4\rho_p d_p g}{3C_D\rho_f}\right)^{0.5} \text{ for } Re_p > 1.0 \tag{6}$$

where $Re_p = \frac{\rho_f V_s d_p}{\mu}$ is the particle Reynolds number. ρ_f is the density of air (1.2 kgm^{-3}). ρ_p is the density of aerosol particle and is assumed to be 1000 kgm^{-3} [29,36]. g is the gravitational acceleration 9.81 ms^{-2}. d_p (m) is the diameter of particle. μ is the viscosity of air ($1.81 \times 10^{-5} kgm^{-1} s^{-1}$). C_D is the drag coefficient. For $Re_p > 1.0$, we have $C_D(Re_p)^2 = \frac{4\rho_p\rho_f g d_p^3}{3\mu^2}$ and it is used to determine the sedimentation velocity graphically [35].

The dry particle size is used in the equations above. It is important to consider the influence of relative humidity on particle deposition because fine hygroscopic dust particles may grow and enlarge by absorbing ambient moisture [37]. In this case, the dry particle size may not be accurate and should be replaced by a wet particle size [38]

$$r_w = \left(\frac{C_1 r_d^{C_2}}{C_3 r_d^{C_4} - \log_{10}[\text{Relative humidity}]} + r_d^3\right)^{1/3} \tag{7}$$

where r_w is the wet particle radius, and $r_d = \frac{d_p}{2}$ is the dry particle radius. For urban aerosol particles, $C_1 = 0.3926$, $C_2 = 3.101$, $C_3 = 4.19 \times 10^{-11}$, and $C_4 = -1.404$. An increase in the diameter of microparticles due to the humidity effect will affect Solar PV soiling by mitigating Brownian diffusion-induced deposition while enhancing inertial impaction and sedimentation-induced deposition as denoted by R_b and V_s. Calculations based on Eq. (7) show that at a relative humidity of 70%, the differences between the dry and wet diameters for 1 and 10 μm particles are 14% and 20% respectively. These changes in the diameter will further lead to 19.8% and 6.7% increases in the deposition velocities of 1 and 10 μm particles, respectively. The effect of relative humidity on solar PV soiling has been rarely included in existing models.

The modelled deposition velocity is with respect to particle deposition onto horizontal surfaces. To account for the impact of the tilt of solar PV panels on particle deposition, the sedimentation velocity (Eq. (1)) is multiplied by the cosine of the tile angle, $\cos\theta$, under the assumption that the sedimentation velocity is the major component affected by the tilt [22]. Solar PV modules generally adopt an optimal tilt angle to maximize the overall energy gain. A simple rule of thumb is to consider the optimal tilt angle as the latitude of a place [39]. Based on this rule, a list of optimum tilt angles for different cities (as considered in the case studies) is given in Table 1.

2.2. Efficiency loss

The efficiency loss (η_{loss}) is defined as the difference between the output efficiencies of solar PV module before (clean status) and after (soiling status) dust accumulation divided by the efficiency before dust accumulation. Linear relationships between the dust deposition density ρ_D ($\frac{g}{m^2}$) and efficiency loss η_{loss} have been reported [40–42]. According to the study by [42], we have

$$\eta_{loss} = 0.0139 \times \rho_D \tag{8}$$

This means that for every $1\frac{g}{m^2}$ of dust deposition, the efficiency of the module degrades by 0.0139%. The dust deposition density ρ_D is estimated based on the deposition velocity V_d by

$$\rho_D = V_d \times C \times 10^{-6} \times \text{Duration (days)} \tag{9}$$

Table 1
List of optimum tilt angles.

City	Optimum tilt angle
Taichung	24°
Tokyo	35°
Hami	43°
Doha	25°
Walkaway	29°
Malibu	34°
Sanlucar la Mayor	37°

$V_d \times C$ is the particle deposition flux. Aerosols are usually polydisperse and have particle sizes that range over two or more orders of magnitudes. If the distribution of particle size is known, it is possible to estimate the particle deposition flux by dividing the distribution into discrete size bins and summing the deposition flux of each size bin. However, the particle size distribution has been rarely reported in the existing literature about solar PV soiling. Alternatively, PV soiling and efficiency loss studies generally used a single concentration metric (*e.g.*, $PM_{2.5}$ and PM_{10}) for the analysis [43]. Hence, for the model analysis in this work, intermediate particle sizes within the range of particle size distribution are used to test the accuracy during model validation.

Rainfall serves as a natural cleaning mechanism for PV panels, but the effectiveness of cleaning was highly contingent upon the quantity of rain. Hammonds et al. [44] suggested that five millimeters of rainfall were sufficient to clean PV panel. But Kimber et al. [45] found that light to moderate rainfall events (< 10 mm) were not sufficient to clean PV panels and a heavy rainfall event of 20 mm could restore an efficiency loss of 40%. In this work, we consider that 80% of particles on solar panels are washed off by large rainfall events (> 10 mm) and 30% of particles are washed off by slight rainfall (< 5 mm).

2.3. Economic analysis

2.3.1. Economics of solar PV soiling and cleaning

One of the major concerns over solar PV soiling is its impact on the economics of solar PV systems. To evaluate the economic impact of solar PV soiling, a relative NPV change ΔNPV% is introduced

$$\Delta NPV\% = \frac{|NPV_0 - NPV_1|}{|NPV_0|} \tag{10}$$

where NPV_0 and NPV_1 denote the NPV of the ideal case without soiling and the actual case with soiling (with or without cleaning). NPV is a way of thinking about converting future income into today's terms and a larger NPV indicates a higher profitability. NPV is calculated as

$$NPV = \sum_{t}^{LT} \frac{C_{it}}{(1+r)^t} - C_0 \tag{11}$$

where C_{it} is the net cash inflow in a year t; C_0 is the total initial investment; LT denotes the lifetime of facilities and is 20 years in this work; $r = 10\%$ is the discount rate accounting for the time value of money for future investment (Ertürk, 2012; Manioğlu & Yılmaz, 2006).

The parameters involved in the economic analysis could potentially have great uncertainties. To account for the uncertainties, a Monte Carlo simulation-based method is adopted following the study by [46]. In this method, uncertain parameters follow triangular distributions with the modes being the nominal value obtained from existing literature. The lower and upper bounds are set as 80% and 120% of the modes. During each run of simulation, a random value of each parameter is sampled from its distribution and plugged into Eqs. (10) and (11) to calculated ΔNPV%. This process was repeated for ten thousand runs, giving rise to a distribution of ΔNPV%.

The cost components consist of a capital cost (*e.g.*, the costs of construction, equipment, tracking system, inverters, and electrical components), operations & maintenance (O&M) cost (*e.g.*, salary and training), and cleaning cost [47]. The benefit components mainly include electricity income. The specific values of the nominal parameters for each city are listed in Table 2.

Manual and machine-assisted methods are available for solar PV cleaning. The machine-assisted method had a cost per cleaning event 80% lower than the manual method [24]. For simplicity, the cleaning cost is considered based on an aggregated value in terms of unit electricity generation. Due to the lack of relevant data for cleaning costs for the considered cities, we apply the ones reported by [24] in the case studies: 0.19 USD/kW for manual cleaning and 0.032 USD/kW for machine-assisted cleaning (Exchange rate: 1 SAR = 0.27 USD). To account for the variation of the efficiency loss with respect to time, a Monte Carlo simulation analysis is used to decide the starting time of cleaning based on which the average efficiency loss is calculated.

A flow diagram of the economic analysis is given in Fig. 2. The overall procedure is: (a) particle deposition velocities were estimated from deposition modelling (Eq. (1)) and were then used to predict the deposition densities (Eq. (9)) and corresponding efficiency losses (Eq. (8)); (b) a uniform distribution was used to randomly determine the starting point in the temporal efficiency loss profile and an average efficiency loss was calculated for a specific cleaning interval; (c) NPV was estimated based on the triangular distributions of parameters (Eq. (11)); (d) the overall calculation was completed if the maximum number of iterations was reached, otherwise, (b)–(d) would be repeated.

2.3.2. Optimum cleaning interval

Based on the theoretical deposition model-based soiling prediction and system-level economic analysis, the optimum cleaning interval could be determined by minimizing the ΔNPV% mean, *i.e.*

$$\min\ (\Delta NPV\%_{mean}) \rightarrow CI_{op} \tag{12}$$

2.4. Case studies

The temporal variations of solar PV efficiency loss by soiling are modelled for seven cities (*i.e.* Taichung, Tokyo, Hami, Malibu, Sanlucar la Mayor, Doha, and Walkaway as shown in Fig. 3) which are world's

Table 2
Nominal parameters for the economic analysis.

Parameter	City						
	Taichung	Tokyo	Hami	Walkaway	Doha	Malibu	Sanlucar la Mayor
Capital (USD/kW)	3760[a]	4300[b]	1500[d]	3100	3900[e]	1950	3100[f]
O&M (%)	0.7%	1.5[c]	1%	1%	1%[c]	0.77%	1.5%[c]
Cleaning (USD/kW)	0.19 (manual) 0.032 (machine-assisted)	0.19 (manual) 0.032 (machine-assisted)	0.19 (manual) 0.032 (machine-assisted)	0.19 (manual)0.032 (machine-assisted)	0.19 (manual) 0.032 (machine-assisted)	0.19 (manual) 0.032 (machine-assisted)	0.19 (manual)0.032 (machine-assisted)
Electricity tariff (USD/kWh)	0.088	0.194	0.15	0.35[f]	0.1	0.12	0.23
References	[24,48,49]	[24,50–52]	[24,53,54]	[24,51,55,56]	[24,57,58]	[24,59,60]	[24,51,61]

[a] Exchange rate: 0.034 USD/NTD.
[b] The value is an average of the ones from [50] and [51].
[c] The world average value is used.
[d] Exchange rate: 0.16 USD/CNY.
[e] The data of Saudi Arabia is used instead.
[f] Exchange rate: 0.79 USD/AUD.

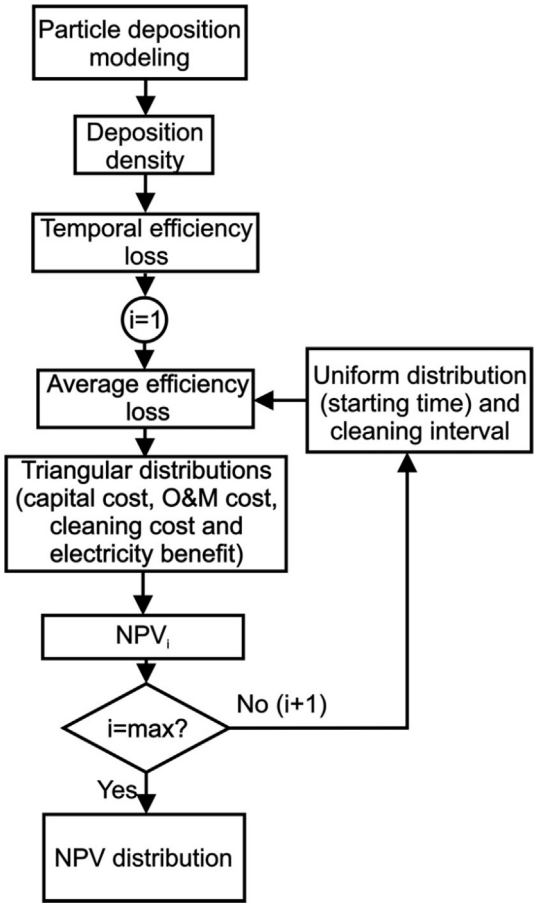

Fig. 2. A flow diagram of the economic analysis.

leading solar PV implementer. They are widely distributed with distinctive climate conditions (*e.g.*, dry California climate in Malibu vs. tropical wet climate in Walkaway), which allows the comparison of the impacts of solar PV soiling across different climate and aerosol conditions. Local meteorological parameters such as monthly relative humidity, rainfall and wind speed are obtained from the World Weather Online website (https://www.worldweatheronline.com/) unless otherwise stated. Aerosol concentration data are from http://aqicn.org/. The weather and aerosol concentration conditions for different cities are listed in Table 3. The temporal variation of efficiency loss is modelled for one year for all the cities except for Doha where 140 days are modelled because over 100% efficiency loss will be resultant for a one-year period. For each city, three tilt angle scenarios are models, *i.e.* optimal tilt angle, optimal tilt angle -10°, and optimal tilt angle $+10^{\circ}$. We consider a solar PV power plant with a capacity of 1 MW (installation size) with an hour-of-daylight of 10 h for each city. The temporal variation of efficiency loss in a year (140 days for Doha) is used as a reference for the economic analysis over the life course of the solar PV power plant. The cleaning interval is varied with a minimal resolution of 1 day for Doha and 7 days for the other cities.

There are various assumptions underlying the calculations: (1) only rainfall washing events are considered and no snow accumulation and wind-induced particle resuspension are considered; (2) rainfall are averaged by dividing the precipitation by the number of rainy days in a month and the frequency is calculated by diving the number of days in a month by the number of rainy days in a month; (3) the particle deposition density is updated on a daily basis; (4) the average diameter of 20 μm by volume for outdoor aerosol from [42] is used to represent the size of particles that are most relevant to solar PV soiling [43].

3. Results and discussion

3.1. Model validation

Model validation is conducted by comparing the model predictions with the reported experimental deposition velocities (*i.e.* [64–70]). The study by [64] includes a relevantly complete list of parameters such as relative humidity, mean wind speed, and aerosol concentration. For the other studies, the missing meteorological data were obtained from World Weather Online website (https://www.worldweatheronline.com/) while the aerosol concentration data $PM_{2.5}$ and PM_{10} were adapted from the World Air Quality website (http://aqicn.org/city/taichung). Other parameters followed [64]. The input parameters for model predictions are listed in Table 4. For TSP (total suspended particulates: 20–50 μm), the particle sizes of 20 and 50 μm were used to model a range of deposition velocity. For PM_{10} (particulate matters smaller than 10 μm), the particle sizes of 5 and 10 μm were used to model a range of deposition velocity. For $PM_{2.5}$, (particulate matter smaller than 2.5 μm) the particle sizes of 1 and 2.5 μm were used to

Fig. 3. Location of the cities considered in the case studies (World map adapted from: www.goethes-farbenlehre.com).

Table 3
Weather and aerosol concentration conditions for different cities.

City		Months											
		Jan.	Feb.	Mar.	Apr.	May	Jun.	Jul.	Aug.	Sep.	Oct.	Nov.	Dec.
Taichung	Relative humidity	71	68	69	68	68	73	70	71	71	73	65	62
	Temperature	20	19	22	28	31	32	33	33	31	31	27	24
	Precipitation (mm)	160	65	253	259	117	368	102	154	268	31	47	15
	Rainy days	22	23	18	21	26	28	25	27	23	14	12	7
	Wind speed (m/s)	8.4	8.8	6.8	4.9	4.9	5.7	5.9	3.4	6.9	5.9	7.6	8.7
	Aerosol concentration ($\mu g/m^3$)	63											
Tokyo	Relative humidity (%)	63	64	65	69	68	76	80	78	83	73	74	65
	Temperature (°C)	8	9	12	17	23	25	28	30	27	21	14	12
	Precipitation (mm)	112	71	85	94	66	125	114	324	219	119	166	48
	Rainy days	12	14	17	19	10	24	17	24	25	20	18	9
	Wind speed (m/s)	3.9	4.7	4.7	5.4	5.3	4.3	3.5	4.3	3.5	3.8	4.2	4.1
	Aerosol Concentration ($\mu g/m^3$)	35											
Hami[a]	Relative humidity (%)	75	74	63	42	35	36	39	36	30	50	62	69
	Temperature (°C)	−9	−7	4	15	18	27	28	26	23	8	0	−3
	Precipitation (mm)	0	0	15	28	12	17	20	17	1	48	31	13
	Rainy days	0	0	4	14	9	6	12	7	1	10	6	4
	Wind speed (m/s)	1.6	1.7	2.5	3.2	4.2	3.1	2.8	2.9	2.3	2.8	2.7	1.9
	Aerosol concentration ($\mu g/m^3$)	125											
Malibu[b]	Relative humidity (%)	67	40	63	55	73	56	59	60	56	53	44	59
	Temperature (°C)	14	18	20	21	19	26	27	25	24	22	21	15
	Precipitation (mm)	95	12	21	11	12	2	0.2	0.1	5	18	21	91
	Rainy days	10	2	7	5	3	1	0	0	5	6	4	11
	Wind speed (m/s)	2.7	4	3	2.8	2.6	2.4	2.4	2.2	2.5	2.7	3.2	3.8
	Aerosol concentration ($\mu g/m^3$)	55											
Sanlucar la Mayor[c]	Relative humidity (%)	77	69	65	65	61	42	38	36	40	56	67	74
	Temperature (°C)	14	14	16	19	22	30	35	34	30	25	16	14
	Precipitation (mm)	79	37	36	78	126	0.2	1.5	1.6	7.3	116	143	42
	Rainy days	15	13	10	15	11	1	3	2	1	7	11	9
	Wind speed (m/s)	3	4.2	2.9	3.1	3.5	3	2.7	2.7	2.5	2.5	2.7	2.9
	Aerosol concentration ($\mu g/m^3$)	34											
Doha[d]	Relative humidity (%)	61	65	52	43	38	37	44	49	47	48	60	62
	Temperature (°C)	20	22	26	29	35	37	39	38	37	32	28	24
	Precipitation (mm)	3	11	26	9	0.4	0	0	0	0	0	11	0
	Rainy days	2	6	13	5	1	0	0	0	0	0	5	0
	Wind speed (m/s)	5.7	5.3	4.8	4.4	5.1	5.6	5.2	3.6	4.7	4.1	4.6	5.5
	Aerosol concentration ($\mu g/m^3$)	200											
Walkaway	Relative humidity (%)	62	49	58	59	61	67	69	68	64	60	55	58
	Temperature (°C)	25	26	25	22	17	15	14	14	15	18	23	24
	Precipitation (mm)	42	1	26	47	35	77	70	49	7	9	4	1.3
	Rainy days	18	2	7	12	7	11	16	15	9	7	5	4
	Wind speed (m/s)	5.5	6.5	6.1	4.9	4.6	4.2	4.9	4.6	5	5.8	6.7	7.2
	Aerosol concentration[e] ($\mu g/m^3$)	17											

[a] The meteorological and TSP data for Hami are not available. The meteorological data for Urumqi is used. The average TSP data for Xinjiang is used [62].
[b] The TSP data for Malibu is not available. The TSP value for the nearest city Los Angeles is used.
[c] The meteorological and TSP data for Sanlucar la Mayor are not available. The meteorological and TSP data for the nearest city Santa Clara, Seville are used.
[d] The aerosol concentration data is adapted from [63].
[e] The TSP data for Walkaway is not available. The TSP data for the nearest city Perth is used.

model a range of deposition velocity.

Fig. 4 shows that model predictions are generally within a five-time difference from the experimental data. A five-time variation in the deposition velocity suggests a five-time difference in the predicted daily efficiency loss. However, taking the case of Taichung as an example and using its meteorological data in January, a five-time variation in the predicted deposition velocity would only change the predicted daily electricity output by 3.4%. Considering that the economic analysis is based on the daily energy output, this may suggest that the model can predict the deposition velocity with satisfactory accuracy for solar PV soiling analysis. For TSP (most relevant to solar PV soiling), its deposition velocity ranges from about 1 to 20 cm/s. Note that the red line connecting two points denote the ranges of experimental data and model predictions and the two end-points denote the experimental and

Table 4
Summary of input parameters for deposition model validation.

Location	Taichung	New York City	Chicago	Berlin	Bursa	Beijing	California
Relative humidity	72%	72%	69%	69%	72%	57%	65%
Temperature (°C)	28	28	28	28	28	28	28
Mean wind speed (ms^{-1})	1.8	1.8	4	4	1.8	3.4	3.85
Aerosol concentration (μgm^{-3})	55 (TSP)	55 (TSP)	53 (PM_{10})	53 (PM_{10})	55 (TSP)	133 ($PM_{2.5}$)	41 ($PM_{2.5}$)

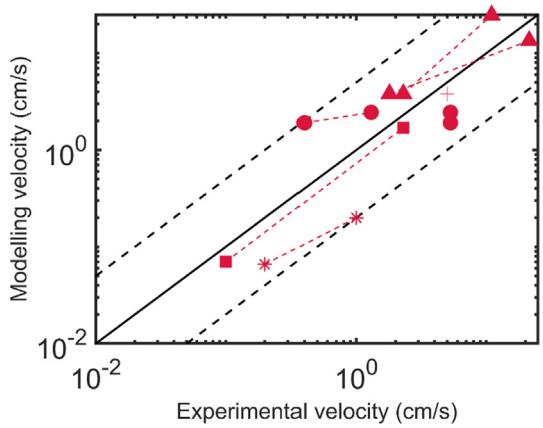

Fig. 4. Model validation. The solid black line denotes the perfect match between modelling predictions and experimental data. The two dotted black lines denote the boundaries for a five-time difference between experimental data and model predictions. The experimental data is from existing studies (*i.e.* [64–70]).

modelling lower and upper bounds.

3.2. Efficiency loss

The temporal variations of the soil-induced efficiency losses of solar PV for different cities are shown in Fig. 5. Overall, the variation of the tilt angle by plus and minus ten degrees change the efficiency loss by 0.01% only.

(a) Taichung

Fig. 5(a) shows that higher efficiency loss occurs during February, and October to December for Taichung, which is attributed to the relatively low precipitation during the months. October to December months have both low precipitation (< 50 mm) and small numbers of rainy days (< 15 days), leading to the most significant efficiency losses during the months: from *ca.* 1% at the beginning of October to *ca.* 25% at the end of December. For the other months, the efficiency loss is consistently less than 2% due to the high and frequent precipitation (The monthly precipitation received during the wet months is about 10–15 times higher than that in the dry months). Without cleaning, an efficiency loss of *ca.* 25% could be incurred after one-year dust soiling.

(b) Hami and Malibu

Without cleaning, Hami and Malibu (Fig. 5(b) and (e)) experience the highest efficiency loss of 36% and 32% in September and August, respectively. The efficiency loss is high during most of the months for both the cities. Hami and Malibu have 'continental desert' and 'Mediterranean' climate, respectively, which are featured by low annual precipitation (*e.g.*, one order of magnitude lower than Taichung). However, compared to Malibu, Hami has higher precipitation and more rainy days, which correspond to the more significant wash-off effect from rainfall for Hami. The aerosol concentration of Hami is double of that of Malibu, which leads to a higher efficiency loss for the case of Hami.

(c) Tokyo and Walkaway

Tokyo and Walkaway (Fig. 5(d) and (g)) have a relatively small efficiency loss over the time compared to the other cities. This is attributed to the combined effect of a lower aerosol concentration and more frequent rainfall. Without cleaning, the efficiency losses for Tokyo and Walkaway after one year soling are 3% and 10%, respectively. Large efficiency loss increases occur in May and December for Tokyo, while they occur on February, and September to December for Walkaway.

(d) Sanlucar la Mayor

Sanlucar la Mayor has low precipitation (< 10 mm) and small numbers of rainy days (< 5 days) during June to September, which leads to a peak efficiency loss of *ca.* 14% during the months. For the other months, the efficiency loss is generally smaller than 5%. Note that Sanlucar la Mayor has a similar aerosol concentration to Tokyo. However, their different precipitation patterns cause the distinctly different efficiency loss variations between the two cities.

(e) Doha

Doha (Fig. 5(c)) experiences the highest efficiency loss (88%) for 140-day soiling because of sparse rainfall as well as a high aerosol concentration associated with sandstorm events. Previous experimental research showed that one-month exposure led to an 18.74% decrease in

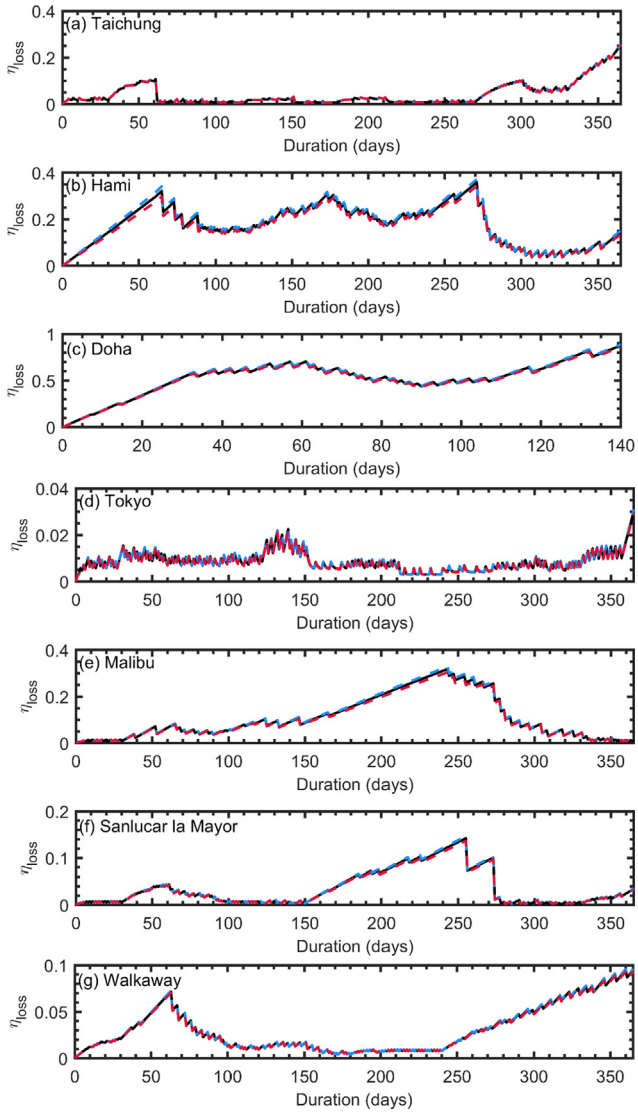

Fig. 5. Temporal variations of soiling-induced efficiency loss for (a) Taichung, (b) Hami, (c) Doha, (d) Tokyo, (e) Malibu, (f) Sanlucar la Mayor, and (g) Walkaway. The black solid lines correspond to the optimal tilt angles (Table 1), while the blue and red dash lines correspond to the optimal tilt angels ± 10°, respectively. (For interpretation of the references to color in this figure legend, the reader is referred to the web version of this article.)

the solar PV efficiency in Baghdad, Iraq [71]. A single sandstorm could reduce the power output of solar PV by 20% in the Eastern province of Saudi Arabia [7]. Rainfall cannot be relied upon for cleaning in such arid places since it occurs occasionally only [7]. Arid areas like the Middle East are characterized by limited precipitation. Coupled with the high amounts of dust, heavy soiling causes significant degradation in efficiency in the region. These places are the prime locations for the construction of concentrated solar plants because they receive high rates of solar irradiation throughout the year [72]. Overall, the efficiency loss (in ascending order) for Tokyo/Walkaway < Taichung < Sanlucar la Mayor < Malibu/Hami < Doha for a one-year period.

3.3. Economic analysis

Fig. 6i shows the variations of relative NPV change with respect to the cleaning interval for different cities. For comparison and illustration, the variations of electricity income loss and cleaning costs with respect to the cleaning interval are also shown (Fig. 6ii). Conventionally, the optimal cleaning interval was determined by matching the cleaning cost with the electricity income loss, while the optimal cleaning interval corresponds to the minimization of the relative NPV change in this work. A list of optimal cleaning intervals and frequencies and NPVs under the optimal interval is given in Table 5. For comparison, the ideal NPVs for the case without soiling (*i.e.* solar PV is always clean) are also listed in Table 5.

Fig. 6 shows that the variation of ΔNPV% has a V shape which was caused by the competitive effect of efficiency loss and cleaning. More frequent cleaning leads to a higher cleaning cost, while less frequent cleaning means a higher efficiency loss and thus electricity income loss, both of which cause a higher NPV reduction. Manual cleaning has a larger ΔNPV% than machine-based cleaning because of the higher unit cost of manual cleaning. Table 5 shows that for the same city, the optimal cleaning intervals for the machine-assisted method are generally shorter than that for the manual method. The electricity income loss firstly decreases as the cleaning interval and then increases. More frequent cleaning does not necessarily cause a lower electricity income loss due to the existence of rainfall cleaning effects. This also suggests that there is an optimal cleaning interval where the electricity income loss is the minimal. For the case of manual cleaning, the optimal cleaning intervals estimated by the method of this work were 7–28 days longer than that by the conventional method which does not lead to the optimized profitability (NPV). For the case of machine-assisted cleaning, the optimal cleaning intervals estimated by the method of this work were not shorter than that by the conventional method for all the cities except for Doha. For Doha, a 6-day shorter interval was estimated by the method of this work.

(a) Taichung

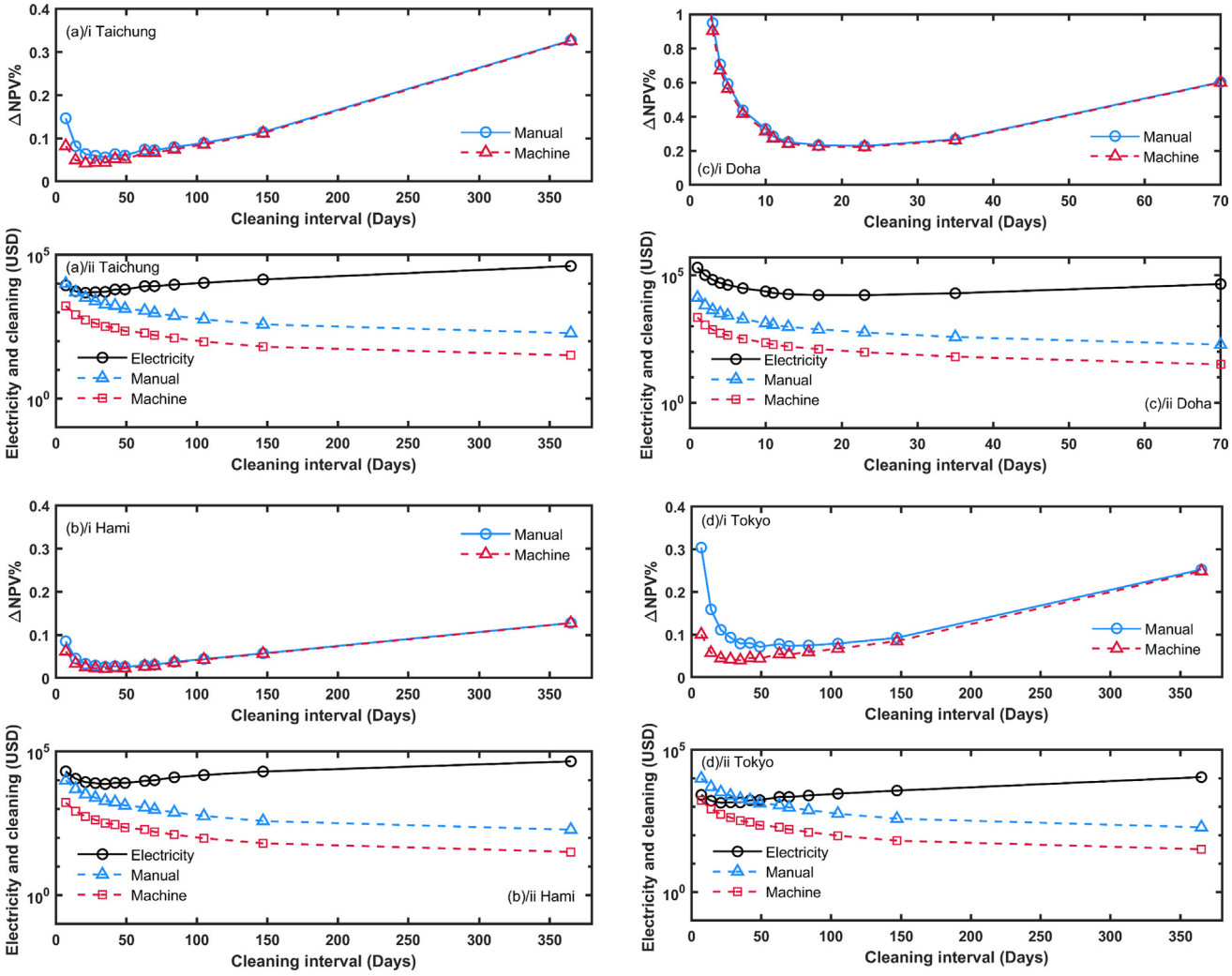

Fig. 6. i: The variations of relative NPV change with respect to the cleaning interval for different cities; ii: The variations of electricity income loss and cleaning costs with respect to the cleaning interval for different cities. "Electricity" denotes the electricity income loss. "Manual" denotes the cost of manual cleaning. "Machine" denotes the cost of machine-assisted cleaning. The installation size is 1 MW.

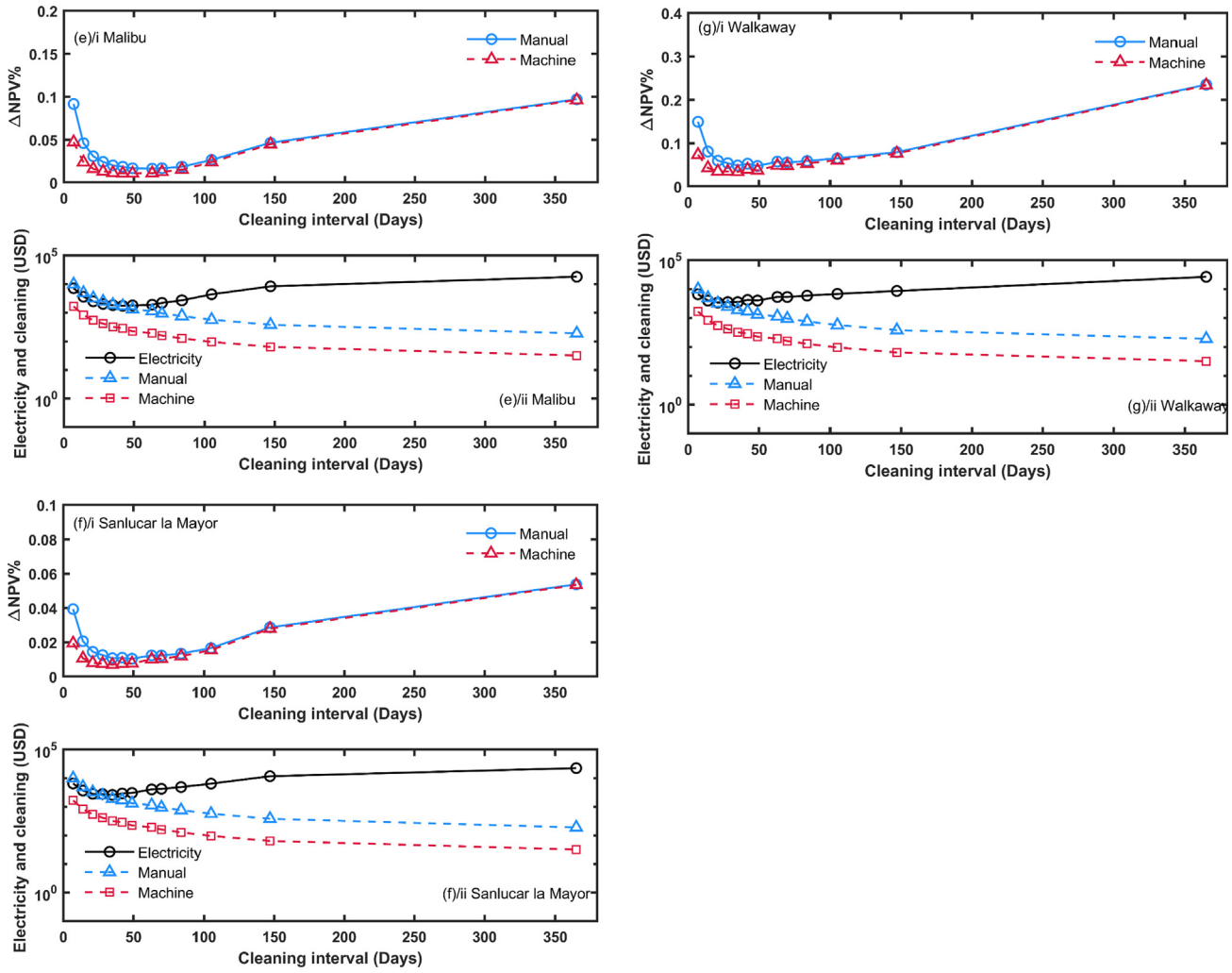

Fig. 6. (*continued*)

For Taichung, ΔNPV% is 14.7% and 32.7% for the manual cleaning interval of 7 and 365 days, respectively, which means that the NPV of the solar PV plant is reduced by 14.7% and 32.7% respectively for the two types of manual cleaning arrangement. For the machine-assisted cleaning, ΔNPV% is 8.2% and 32.6% under the interval of 7 and 365 days. Hence, the method (*i.e.* manual vs. machine) of cleaning plays a bigger role for more frequent cleaning due to the increase in its weight in the overall cost. The optimal cleaning interval corresponds to the minimal ΔNPV%. As listed in Table 5, it is 32 and 21 days, and the corresponding ΔNPV% is 5.6% and 4.3%, respectively, for manual and machine-assisted cleaning for Taichung. By setting the optimal cleaning interval for the manual and machine-assisted methods, respectively, the NPV difference between the methods is only 0.01 million USD. The conventional way of optimal cleaning interval estimation (minimizing the difference between cleaning cost and electricity income loss) produces a much shorter cleaning interval for both the methods (14 days for manual and 21 days for machine).

(b) Hami

The relative NPV change of Hami is smaller than that of Taichung because of its higher absolute value of NPV. Due to the low capital and

Table 5
A list of optimal cleaning intervals, and NPVs under the optimal interval (installation size: 1 MW).

City	This work: Interval (days)		Conventional: Interval (days)		NPV (million USD)[a]		NPV (million USD)
	Manual	Machine	Manual	Machine	Manual	Machine	Ideal
Taichung	35	21	14	21	−1.31 (0.39[b])	−1.30 (0.39)	−1.25 (0.39)
Tokyo	49	35	42	14	1.15 (0.63)	1.16 (0.63)	1.18 (0.63)
Hami	35	35	21	35	2.95 (0.40)	2.97 (0.40)	3.03 (0.41)
Doha	23	17	17	23	−1.28 (0.42)	−1.27 (0.42)	−1.13 (0.43)
Malibu	70	49	42	35	1.62 (0.35)	1.63 (0.35)	1.65 (0.35)
Sanlucar la Mayor	49	35	28	35	3.60 (0.65)	3.62 (0.65)	3.64 (0.66)
Walkaway	49	35	28	21	1.25 (0.46)	1.26 (0.46)	1.30 (0.47)

[a] NPVs correspond to the optimal cleaning intervals predicted by this work.
[b] Data in the brackets denote standard deviations.

O&M costs (Table 2), Hami has a positive average NPV of 3.03 million USD. The large absolute NPV also indirectly lessens the impact of cleaning, which causes a similar optimal cleaning interval between the two methods, *i.e.* 35 days. The relative NPV changes under the cleaning interval of 7, 35, and 365 days are 8.6%, 2.6%, and 12% for manual cleaning and 6.2%, 2.2%, and 12% for machine-assisted cleaning. Based on the conventional method, a shorter optimal cleaning interval of 21 days is obtained for manual cleaning while the same optimal cleaning interval (35 days) is obtained for machine-assisted cleaning.

(c) Doha

For Doha, the relative NPV change varies from around 20% at the optimal cleaning intervals (23 days for manual and 17 days for machine) to over 100% at the cleaning interval less than 3 days, which suggests the significant impact of soiling and relevant cleaning on the economics of solar PV plants in arid areas like Doha. Compared to the other cities, Doha is more sensitive to the cleaning interval and has much shorter cleaning intervals due to the larger soiling-induced solar PV efficiency loss. The optimal cleaning intervals for manual and machine-assisted cleaning corresponds to the relative NPV changes of 21% and 19%, respectively. The optimal cleaning intervals by the conventional method are 17 and 23 days for manual and machine-assisted cleaning, respectively.

(d) Tokyo, Walkaway and Sanlucar la Mayor

Tokyo has the same optimal cleaning intervals (49 days for manual and 35 days for machine) as Sanlucar la Mayor and Walkaway. For manual cleaning, the optimal intervals by the conventional method are 42, 28, and 28 days, for Tokyo, Sanlucar la Mayor, and Walkaway. For machine-assisted cleaning, the optimal intervals by the conventional method are 14, 35, and 21 days for Tokyo, Sanlucar la Mayor, and Walkaway. The relative NPV change at the same cleaning interval for Sanlucar la Mayor is only around a fifth to a tenth of that for Tokyo and Walkaway.

(e) Malibu

Malibu has the longest cleaning intervals: 70 days for manual and 49 days for machine which correspond to the relative NPV changes of 1.7% and 1.1%. However, the efficiency loss for Malibu is not the largest as shown in Fig. 4. This suggests that the optimal cleaning intervals are not only determined by the soiling-induced efficiency degradation but also the system's overall cost and benefit components, which re-emphasizes that it is critical to estimate the optimal cleaning interval from the perspective of the overall system economics. The conventional method predicts the optimal cleaning intervals of 42 and 35 days for manual and machine-assisted cleaning. Overall, the NPV-based system level method generally predicts longer optimal intervals than the conventional method for both cleaning methods.

3.4. Future development

This work adopted the average efficiency loss model (Eq. (8)) that was obtained based on the experimental data for three different modules: *i.e.* mono-crystalline silicon with white glass as the surface material, poly-crystalline silicon with epoxy as the surface material, and amorphous silicon with white glass as the surface material [42]. However, the efficiency loss was also dependent on the types of PV modules and soiling particles, and solar density [40]. For example, a poly-crystalline silicon module packaged with epoxy degraded faster than a mono-crystalline silicon module with a white glass surface under the same deposition density [42]. For a similar type of module and deposition density, the efficiency reduction was the largest for red soil, followed by limestone, ash, and natural air pollutant, respectively, as a result of composition differences [73]. New models that could differentiate the effects of the factors need to be developed for more specific prediction.

For highly soiling cases such as the one of Doha, it is worth noting there might be two stages of fouling [74]. In the “early stage of fouling” single-particle deposition and re-suspension is at an equilibrium state and the efficiency loss increases with the particle deposition density [75]. As more particles accumulate without being removed *e.g.*, via rainfall, there occurs the “later stage of fouling” where multilayer formation and clogging occurs [74]. In this case, new dust particles will deposit and settle on existing particles. Although ρ_D increases, it might not reduce the efficiency further since the surface is ‘saturated’ by particles. Hence, the efficiency loss will ‘flatten’ and plateau off instead of increasing further [76]. The extent of this saturation effect is still unknown and thus not included in this work, which warrant future studies. Finally, it will be desirable to incorporate the method of this work into the operation and management systems of existing solar PV plants to design optimal operation and management schemes.

4. Conclusions

This work improves the current ability of predicting temporal solar photovoltaic soiling using the upgraded mechanistic model. It introduces a new method to predict the optimal interval of solar photovoltaic cleaning based on a combination of the mechanistic model and system-level economic analysis (relative net-present value). The method could potentially be incorporated into the operation and management systems of existing solar photovoltaic plants. This will allow operators to make timely and informed decisions about when to conduct the cleaning to improve the profitability of solar net-present value systems. Based on the method, the soiling-induced efficiency and economic losses of solar photovoltaic modules in seven cities (*i.e.*, Taichung, Tokyo, Hami, Malibu, Sanlucar la Mayor, Doha, and Walkaway) were compared. It was found that varying the tilt angle by plus and minus ten degrees changed the efficiency loss by 0.01% only. Overall, the efficiency loss (in ascending order) for Tokyo/Walkaway < Taichung < Sanlucar la Mayor < Malibu/Hami < Doha for a one-year period. The predicted optimal cleaning interval ranges from 23 to 70 days and 17 to 49 days for the manual and machine-assisted cleaning methods, respectively. Malibu has longest optimal cleaning intervals (70 days for manual cleaning and 49 days for machine-assisted cleaning) that leads to the relative net-present value changes of 1.7% and 1.1%. Doha has the shortest optimal cleaning intervals (23 days for manual cleaning and 17 days for machine-assisted cleaning) that leads to the relative net-present value changes of 21% and 19%.

Acknowledgment

This research program is funded by the National Research Foundation (NRF), Prime Minister’s Office, Singapore under its Campus for Research Excellence and Technological Enterprise (CREATE) program. Grant Number R-706-001-101-281, National University of Singapore.

References

[1] Conti J, Holtberg P, Diefenderfer J, LaRose A, Turnure JT, Westfall L. International energy outlook 2016 with projections to 2040. USDOE Energy Information Administration (EIA), Washington, DC (United States). Office of Energy Analysis; 2016.
[2] Al Garni HZ, Awasthi A. Solar PV power plant site selection using a GIS-AHP based approach with application in Saudi Arabia. Appl Energy 2017;206:1225–40.
[3] Khatib T, Kazem H, Sopian K, Buttinger F, Elmenreich W, Albusaidi AS. Effect of dust deposition on the performance of multi-crystalline photovoltaic modules based on experimental measurements. Int J Renew Energy Res 2013;3:850–3.
[4] Cabanillas R, Munguía H. Dust accumulation effect on efficiency of Si photovoltaic modules. J Renew Sustainable Energy 2011;3:043114.
[5] AlBusairi HA, Möller HJ. Performance evaluation of CdTe PV modules under natural

outdoor conditions in Kuwait. 25th European solar energy conference and exhibition/5th world conference on photovoltaic energy conversion, Valencia, Spain, September 2010. p. 6–10.
[6] Piliougine M, Cañete C, Moreno R, Carretero J, Hirose J, Ogawa S, et al. Comparative analysis of energy produced by photovoltaic modules with anti-soiling coated surface in arid climates. Appl Energy 2013;112:626–34.
[7] Adinoyi MJ, Said SA. Effect of dust accumulation on the power outputs of solar photovoltaic modules. Renewable Energy 2013;60:633–6.
[8] Jamil WJ, Rahman HA, Shaari S, Salam Z. Performance degradation of photovoltaic power system: Review on mitigation methods. Renew Sustain Energy Rev 2017;67:876–91.
[9] Sarver T, Al-Qaraghuli A, Kazmerski LL. A comprehensive review of the impact of dust on the use of solar energy: History, investigations, results, literature, and mitigation approaches. Renew Sustain Energy Rev 2013;22:698–733.
[10] Masa-Bote D, Castillo-Cagigal M, Matallanas E, Caamaño-Martín E, Gutiérrez A, Monasterio-Huelín F, et al. Improving photovoltaics grid integration through short time forecasting and self-consumption. Appl Energy 2014;125:103–13.
[11] Buffat R, Grassi S, Raubal M. A scalable method for estimating rooftop solar irradiation potential over large regions. Appl Energy 2018;216:389–401.
[12] Rovelli G, Miles RE, Reid JP, Clegg SL. Accurate measurements of aerosol hygroscopic growth over a wide range in relative humidity. J Phys Chem A 2016;120:4376–88.
[13] Lu H, Lu L, Wang Y. Numerical investigation of dust pollution on a solar photovoltaic (PV) system mounted on an isolated building. Appl Energy 2016;180:27–36.
[14] Said SA, Hassan G, Walwil HM, Al-Aqeeli N. The effect of environmental factors and dust accumulation on photovoltaic modules and dust-accumulation mitigation strategies. Renew Sustain Energy Rev 2018;82:743–60.
[15] Wang J, Gong H, Zou Z. Modeling of dust deposition affecting transmittance of PV modules. J Clean Energy Technol 2017;5:217–21.
[16] Elminir HK, Ghitas AE, Hamid R, El-Hussainy F, Beheary M, Abdel-Moneim KM. Effect of dust on the transparent cover of solar collectors. Energy Convers Manage 2006;47:3192–203.
[17] Mejia FA, Kleissl J. Soiling losses for solar photovoltaic systems in California. Sol Energy 2013;95:357–63.
[18] Lu H, Zhao W. Effects of particle sizes and tilt angles on dust deposition characteristics of a ground-mounted solar photovoltaic system. Appl Energy 2018;220:514–26.
[19] Pavan AM, Mellit A, De Pieri D. The effect of soiling on energy production for large-scale photovoltaic plants. Sol Energy 2011;85:1128–36.
[20] Hammad B, Al-Abed M, Al-Ghandoor A, Al-Sardeah A, Al-Bashir A. Modeling and analysis of dust and temperature effects on photovoltaic systems' performance and optimal cleaning frequency: Jordan case study. Renew Sustain Energy Rev 2017.
[21] Moghimi M, Ahmadi G. Wind barriers optimization for minimizing collector mirror soiling in a parabolic trough collector plant. Appl Energy 2018;225:413–23.
[22] Jiang Y, Lu L, Lu H. A novel model to estimate the cleaning frequency for dirty solar photovoltaic (PV) modules in desert environment. Sol Energy 2016;140:236–40.
[23] You R, Zhao B, Chen C. Developing an empirical equation for modeling particle deposition velocity onto inclined surfaces in indoor environments. Aerosol Sci Technol 2012;46:1090–9.
[24] Jones RK, Baras A, Al Saeeri A, Al Qahtani A, Al Amoudi AO, Al Shaya Y, et al. Optimized cleaning cost and schedule based on observed soiling conditions for photovoltaic plants in central Saudi Arabia. IEEE J Photovolt 2016;6:730–8.
[25] Picotti G, Borghesani P, Cholette M, Manzolini G. Soiling of solar collectors–Modelling approaches for airborne dust and its interactions with surfaces. Renew Sustain Energy Rev 2017.
[26] Slinn S, Slinn W. Predictions for particle deposition on natural waters. Atmos Environ 1980;14:1013–6.
[27] Giard D, Bazile E. Implementation of a new assimilation scheme for soil and surface variables in a global NWP model. Mon Weather Rev 2000;128:997–1015.
[28] Fernando HJ. Handbook of environmental fluid dynamics, volume two: systems, pollution, modeling, and measurements. CRC Press; 2012.
[29] Nho-Kim E-Y, Michou M, Peuch V-H. Parameterization of size-dependent particle dry deposition velocities for global modeling. Atmos Environ 2004;38:1933–42.
[30] Jarraud M. Guide to meteorological instruments and methods of observation (WMO-No. 8). Geneva, Switzerland: World Meteorological Organisation; 2008.
[31] Aluko O, Noll KE. Deposition and suspension of large, airborne particles. Aerosol Sci Technol 2006;40:503–13.
[32] Boyle L, Flinchpaugh H, Hannigan M. Assessment of PM dry deposition on solar energy harvesting systems: measurement–model comparison. Aerosol Sci Technol 2016;50:380–91.
[33] Zhang L, Gong S, Padro J, Barrie L. A size-segregated particle dry deposition scheme for an atmospheric aerosol module. Atmos Environ 2001;35:549–60.
[34] Knippertz P, Stuut J-BW. Introduction. Mineral Dust. Springer; 2014. p. 1–14.
[35] Rhodes MJ. Introduction to particle technology. John Wiley & Sons; 2008.
[36] Hinds WC. Aerosol technology: properties, behavior, and measurement of airborne particles. John Wiley & Sons; 2012.
[37] Ng DHL, Li R, Raghavan SV, Liong S-Y. Investigating the relationship between Aerosol Optical Depth and Precipitation over Southeast Asia with Relative Humidity as an influencing factor. Sci Rep 2017;7:13395.
[38] Gerber HE. Relative-humidity parameterization of the Navy Aerosol Model (NAM). Naval Research Lab Washington DC; 1985.
[39] Lave M, Kleissl J. Optimum fixed orientations and benefits of tracking for capturing solar radiation in the continental United States. Renew Energy 2011;36:1145–52.
[40] Sayyah A, Horenstein MN, Mazumder MK. Energy yield loss caused by dust deposition on photovoltaic panels. Sol Energy 2014;107:576–604.
[41] Brown K, Narum T, Jing N. Soiling test methods and their use in predicting performance of photovoltaic modules in soiling environments. Photovoltaic Specialists Conference (PVSC), 2012 38th IEEE. IEEE; 2012. p. 001881–5.
[42] Jiang H, Lu L, Sun K. Experimental investigation of the impact of airborne dust deposition on the performance of solar photovoltaic (PV) modules. Atmos Environ 2011;45:4299–304.
[43] Figgis B, Ennaoui A, Ahzi S, Rémond Y. Review of PV soiling particle mechanics in desert environments. Renew Sustain Energy Rev 2017;76:872–81.
[44] Hammond R, Srinivasan D, Harris A, Whitfield K, Wohlgemuth J. Effects of soiling on PV module and radiometer performance. Photovoltaic specialists conference, 1997, conference record of the twenty-sixth IEEE. IEEE; 1997. p. 1121–4.
[45] Kimber A, Mitchell L, Nogradi S, Wenger H. The effect of soiling on large grid-connected photovoltaic systems in California and the southwest region of the United States. Photovoltaic energy conversion, conference record of the 2006 IEEE 4th world conference on. IEEE; 2006. p. 2391–5.
[46] You S, Wang W, Dai Y, Tong YW, Wang C-H. Comparison of the co-gasification of sewage sludge and food wastes and cost-benefit analysis of gasification-and incineration-based waste treatment schemes. Bioresour Technol 2016;218:595–605.
[47] Harder E, Gibson JM. The costs and benefits of large-scale solar photovoltaic power production in Abu Dhabi, United Arab Emirates. Renew Energy 2011;36:789–96.
[48] Lin J-X, Wen P-L, Feng C-C, Lin S-M, Ko F-K. Policy target, feed-in tariff, and technological progress of PV in Taiwan. Renew Sustain Energy Rev 2014;39:628–39.
[49] Yang F, Sun C, Huang G. Study on cross-strait energy cooperation under the new circumstance. J Cleaner Prod 2018.
[50] Pereira JP, Parady GT, Dominguez BC. Japan's energy conundrum: Post-Fukushima scenarios from a life cycle perspective. Energy Policy 2014;67:104–15.
[51] Baurzhan S, Jenkins GP. Off-grid solar PV: Is it an affordable or appropriate solution for rural electrification in Sub-Saharan African countries? Renew Sustain Energy Rev 2016;60:1405–18.
[52] Byrne J, Taminiau J, Kim KN, Lee J, Seo J. Multivariate analysis of solar city economics: Impact of energy prices, policy, finance, and cost on urban photovoltaic power plant implementation. Wiley Interdisciplinary Rev: Energy Environ 2017;6.
[53] Yuan J, Sun S, Zhang W, Xiong M. The economy of distributed PV in China. Energy 2014;78:939–49.
[54] Ye L-C, Rodrigues JF, Lin HX. Analysis of feed-in tariff policies for solar photovoltaic in China 2011–2016. Appl Energy 2017;203:496–505.
[55] Hinkley J, Hayward J, McNaughton R, Gillespie R, Matsumoto A, Watt M, et al. Cost assessment of hydrogen production from PV and electrolysis. CSIRO Australia 2016.
[56] Agnew S, Smith C, Dargusch P. Causal loop modelling of residential solar and battery adoption dynamics: A case study of Queensland, Australia. J Clean Prod 2018;172:2363–73.
[57] Al Garni H, Kassem A, Awasthi A, Komljenovic D, Al-Haddad K. A multicriteria decision making approach for evaluating renewable power generation sources in Saudi Arabia. Sustainable Energy Technol Assess 2016;16:137–50.
[58] Krarti M, Ali F, Alaidroos A, Houchati M. Macro-economic benefit analysis of large scale building energy efficiency programs in Qatar. International Journal of Sustainable. Built Environ 2017.
[59] Fu R, Feldman DJ, Margolis RM, Woodhouse MA, Ardani KB. US solar photovoltaic system cost benchmark: Q1 2017. Golden, CO (United States): National Renewable Energy Laboratory (NREL); 2017.
[60] Marrero GA, Puch LA, Ramos-Real FJ. Mean-variance portfolio methods for energy policy risk management. Int Rev Econ Finance 2015;40:246–64.
[61] Ondraczek J, Komendantova N, Patt A. WACC the dog: The effect of financing costs on the levelized cost of solar PV power. Renew Energy 2015;75:888–98.
[62] Zhang X-X, Sharratt B, Chen X, Wang Z-F, Liu L-Y, Guo Y-H, et al. Dust deposition and ambient PM_{10} concentration in central Asia: Spatial and temporal variability. Atmos Chem Phys 2016;17:1699–711.
[63] Saraga D, Maggos T, Sadoun E, Fthenou E, Hassan H, Tsiouri V, et al. Chemical characterization of indoor and outdoor particulate matter ($PM_{2.5}$, PM_{10}) in Doha, Qatar. Aerosol Air Qual Res 2017;17:1156–68.
[64] Fang G-C, Chiang H-C, Chen Y-C, Xiao Y-F, Zhuang Y-J. Particulates and metallic elements monitoring at two sampling sites (harbor, airport) in Taiwan. Environ Forensics 2014;15:296–305.
[65] Vong RJ, Vong IJ, Vickers D, Covert DS. Size-dependent aerosol deposition velocities during BEARPEX'07. Atmos Chem Phys 2010;10:5749–58.
[66] Sun F, Yin Z, Lun X, Zhao Y, Li R, Shi F, et al. Deposition velocity of $PM_{2.5}$ in the winter and spring above deciduous and coniferous forests in Beijing, China. PloS One 2014;9:e97723.
[67] Tasdemir Y, Kural C. Atmospheric dry deposition fluxes of trace elements measured in Bursa, Turkey. Environ Pollut 2005;138:462–72.
[68] Langner M, Kull M, Endlicher WR. Determination of PM_{10} deposition based on antimony flux to selected urban surfaces. Environ Pollut 2011;159:2028–34.
[69] Holsen TM, Noll KE, Fang GC, Lee WJ, Lin JM, Keeler GJ. Dry deposition and particle size distributions measured during the Lake Michigan urban air toxics study. Environ Sci Technol 1993;27:1327–33.
[70] Raynor GS. Experimental studies of pollen deposition to vegetated surfaces. Atmosphere-Surface Exchange Particulate Gaseous Pollutants 1974:264–79.
[71] Saidan M, Albaali AG, Alasis E, Kaldellis JK. Experimental study on the effect of dust deposition on solar photovoltaic panels in desert environment. Renewable Energy 2016;92:499–505.
[72] Herrmann J, Slamova K, Glaser R, Köhl M. Modeling the soiling of glazing materials in arid regions with geographic information systems (GIS). Energy Procedia 2014;48:715–20.
[73] Kaldellis J, Kapsali M. Simulating the dust effect on the energy performance of photovoltaic generators based on experimental measurements. Energy 2011;36:5154–61.
[74] Henry C, Minier J-P, Lefèvre G. Towards a description of particulate fouling: From single particle deposition to clogging. Adv Colloid Interface Sci 2012;185:34–76.
[75] Adhiwidjaja I, Matsusaka S, Yabe S, Masuda H. Simultaneous phenomenon of particle deposition and reentrainment in charged aerosol flow—effects of particle charge and external electric field on the deposition layer. Adv Powder Technol 2000;11:221–33.
[76] Molki A. Dust affects solar-cell efficiency. Phys Educ 2010;45:456–8.